Proyecciones Journal of Mathematics
Vol. 35, N^o 1, pp. 11-31, March 2016.
Universidad Católica del Norte
Antofagasta - Chile
DOI: 10.4067/S0716-09172016000100002

Similarity Solution of Spherical Shock Waves - Effect of Viscosity

Narsimhulu Dunna
BITS-Pilani, India

Addepalli Ramu
BITS-Pilani, India
and
Dipak Kumar Satpathi
BITS-Pilani, India
Received : March 2015. Accepted : March 2016

Abstract

In this paper we investigated self-similar solutions for Magneto Hydrodynamic shock waves for the equation of state of Mie-Gruneisen type. Solutions are obtained numerically and the effect of viscosity (K) *and the non-idealness parameter* (d) *on the self-similar solutions are studied in detail. The findings confirmed that, the non-idealness parameter and the viscosity parameter have major effect on the shock strength and the flow variables. All discontinuities of the physical parameters are removed by the viscosity and complete flow field depends upon the magnitude of the viscosity. The obtained results are in good agreement with the results obtained by some of the researchers. All the analysis is presented pictorially in this paper.*

Keywords : *Similarity solutions, Shock waves, Magnetogasdynamics, Viscosity, Rankine-Hugoniot condition, Mie-Gruneisen type, Numerical solution.*

Mathematics Subject Classification (MSC) : *76M55, 76L05, 76W05.*

1. Introduction

Shockwaves are very common phenomenon in the supersonic flow of any fluid. Shock process occurs naturally that are related to hydrodynamics, aerodynamics, astrophysics, nuclear engineering and space science. Shock waves are mathematically treated as discontinuities. Shock wave is not a true physical discontinuity, but a very narrow transition zone whose thickness is of the order of a few molecular mean-free paths. In a shocked medium, particles behind the shock front experience compressive as well as shear forces thus the particles move away from their equilibrium position. The similarity solutions of converging spherical and cylindrical shock wave problems with different equation of states (EOS) were investigated by several authors [1, 6, 7, 9, 12, 15, 19, 22, 24]. The existence and effects of the viscous forces for the similarity solutions to shock wave problems were studied by several researchers [10, 17, 21, 28]. Landau and Lifshitz [14] and Zel'dovich and Raizer [27] have studied the entropy production in a viscous medium and developed an analytical model for the shock process based on Hugoniot curves considering the effects of viscosity and heat conduction. The role of viscosity in physics and mathematical investigation of model problems suggest that the presence of viscosity implies the existence of a continuous, differentiable solution. This mathematical theory does not guarantee this in general. The actual formulation of artificial viscosity introduced by Von Neumann and Richtmyer [25] involved adding a viscosity term to the momentum equation, that augments the pressure in the instance there is shock compression and is independent of shock strength. The new system will satisfy the Rankine-Hugoniot jump conditions (Caramana et al. [4]) in the shock region and has little effect outside the shock layer. The resistance to variations in distribution of cohesive forces in fluids experienced result in removing the inhomogeneities in velocities. These types of resistances result in the phenomenon of viscosity in fluid motions Blazek [3]. This viscosity effect was found to be one of the most important effects in the equations of motion. The shock heating of solar corona discussed by Orta et al. [18] have shown that the shock thickness and profile depend on viscosity and resistivity and as a consequence heating ultimately occurs. Ballai et al. [2] in the study of dispersive shock waves concluded that the effect of dispersion will alter the amplitude and propagation speed of a shock wave and also discussed in detail the viscosity effect. The supersonic flows exhibit an important property i.e., the coexistence of shock waves with viscous effects for many fluid dynamic systems Korzhov et al.

[13]. Also the viscous interactions of solar wind stream were studied by Korzhov et al. [13]. The study of interplanetary shock waves are produced due to coronal mass ejection and solar winds and study of these is very important for space weather purposes. The shock waves occur where the solar wind changes from being supersonic to being subsonic. In the supersonic regime of compressible gas flow the interaction of shock waves with viscosity is a very important problem. Mathematically this can be approximated to a hydrodynamic case. Several astrophysical and geophysical phenomena occur due to the Magnetohydrodynamic (MHD) shockwaves. Detailed understanding of the evolution of disturbances in viscous flow and its mechanisms in MHD is essential for the development of efficient methods for controlling different types of flows encountered by the hypersonic flying objects. Some of the applications by the application of external magnetic field are drag reduction in duct flows, design of coolant blankets for fusion reactors, control of turbulence of immersed jets during continuous casting of steel, advanced flow control schemes for hypersonic vehicles and missiles.

1.1. Goal of present work

The main purpose of this paper is to describe complete mechanism of shock wave problem, which include viscous terms and study the dissipation effects on the propagation of shock waves including viscosity under the effect of magnetic field. Also to study and confirm the effect of (i) the non-idealness parameter and the viscosity parameters on the shock strength and the flow variables respectively (ii) effect of discontinuities of the physical parameters due to viscosity and (iii) complete flow field depending on the magnitude of the viscosity. To define this type of shock process spherically symmetric conservation equations are considered. The viscosity term (suggested by Von Neumann and Richtmyer [25]) is included into the hydrodynamic equations for spherically symmetric flow. The main advantage of artificial viscosity approach is its simplicity thereby high computational efficiency and oscillations in the flow profiles dampen and the smoothness in the profiles increases.

2. Formulation of the Problem

The viscosity term suggested by is included into the hydrodynamic equations for spherically symmetric flow in magnetogasdynamics regime, can be written in Eulerian form [8, 14, 20, 25, 26, 27] as

$$\frac{\partial \rho}{\partial t} + \frac{\partial(\rho u)}{\partial r} + 2\frac{\rho u}{r} = 0 \tag{2.1}$$

$$\frac{\partial u}{\partial t} + u\frac{\partial u}{\partial r} + \frac{1}{\rho}(\frac{\partial q}{\partial r} + \frac{\partial p}{\partial r} + \frac{\partial h}{\partial r}) = 0 \tag{2.2}$$

$$\frac{\partial e}{\partial t} + u\frac{\partial e}{\partial r} - \frac{(p+q)}{\rho^2}\left[\frac{\partial \rho}{\partial t} + u\frac{\partial \rho}{\partial r}\right] \tag{2.3}$$

$$\frac{\partial h}{\partial t} + u\frac{\partial h}{\partial r} + 2h\frac{\partial u}{\partial r} + \frac{4hu}{r} = 0 \tag{2.4}$$

where r and t are independent space and time coordinates ρ, u, p, q and e are density, velocity, pressure, artificial viscosity and internal energy per unit mass respectively and $h = \frac{\mu H^2}{2}$ is the magnetic pressure, H and μ being magnetic field strength and the magnetic permeability respectively. The shock position is given by $R_s(t)$ and its velocity $D = \frac{dR_s(t)}{dt}$. Originally Von Neumann and Richtmyer [25] proposed the following expression for the viscosity term:

$$q = \begin{cases} -\rho K^2(\triangle x)^2 \left(\frac{\partial u}{\partial x}\right)^2, & \text{if } \frac{\partial u}{\partial x} < 0 \text{ or } \frac{\partial \rho}{\partial t} > 0 \\ 0 & \text{otherwise} \end{cases}$$

u is the fluid velocity, ρ is the density, $\triangle x$ is spacial interval and K is a constant parameter whose value is conveniently adjusted in every numerical experiment. This parameter K controls the number of zones in which the shock waves are spread. The form of q adopted for the present problem is consistent with Richard Latter [21] requirements and is

$$q = \frac{1}{2}K^2\rho r^2 \frac{\partial u}{\partial r}\left(|\frac{\partial u}{\partial r}| - \frac{\partial u}{\partial r}\right) \tag{2.5}$$

The expression for q denotes a non-linear dissipative mechanism, which is effective in the shock layer and negligible elsewhere.

2.1. Boundary conditions

The boundary conditions at shock front due to Rankine-Hugoniot jump relations, under the strong shock limit can be written into the following

form [23, 27]

$$\rho_1 = \rho_0\beta,\ u_1 = \left(1-\frac{1}{\beta}\right)D,\ p_1 = \left(1-\frac{1}{\beta}-\frac{c_0\beta^2}{2}\right)\rho_0 D^2,\ h_1 = \frac{c_0\beta^2}{2}\rho_0 D^2 \tag{2.6}$$

The equation of state (EOS) is of Mie-Gruneisen type [19] of the following form

$$p = [\Gamma(\rho/\rho_0) - 1]\rho e - \Pi(\rho/\rho_0) \tag{2.7}$$

where Γ and Π are functions to be determined according to the EOS under consideration and Each Γ and Π gives different EOS. Using the strong shock relations (2.6) in equation (2.7) we get

$$2 - \frac{c_0\beta^3}{\beta-1} + \frac{2\beta}{\beta-1}\Pi(\beta) = (\beta-1)(\Gamma(\beta)-1) \tag{2.8}$$

where β is the measure of shock strength.

2.2. Transformation of basic equations

We consider a set of suitable similarity transformations

$$\rho = \rho_0\psi(\xi),\quad u = D\phi(\xi),\quad p = \rho_0 D^2 f(\xi),\quad h = \rho_0 D^2 l(\xi),\quad q = \rho_0 D^2 g(\xi) \tag{2.9}$$

where $\xi = \frac{r}{R}$, ξ is the similarity variable and $R = A(t)^\alpha$ (shock propagation follows a power law), ψ, ϕ, f, l and g are dimensionless density, velocity, pressure, magnetic pressure and viscosity term (which are functions of ξ) respectively. In general these terms are termed as reduced functions. Along with the reduced functions we consider a similar set of transformations for convenience such as,

$$\psi(\xi) = \Psi(\xi),\ \phi(\xi) = \frac{\xi}{\alpha}\Phi(\xi),\ f(\xi) = \frac{\xi^2}{\alpha^2}F(\xi),\ l(\xi) = \frac{\xi^2}{\alpha^2}L(\xi),\ g(\xi) = \frac{\xi^2}{\alpha^2}G(\xi) \tag{2.10}$$

where Ψ, Φ, F, L and G are new unknown reduced functions for the reduced density, velocity, pressure, magnetic pressure and viscosity term functions

respectively. Using the transformations (2.9) and (2.10), the equations (2.1)−(2.5) can be written in the following non dimensional form:

$$(\Phi-\alpha)\frac{d\ln\Psi}{d\ln\xi}+\frac{d\Phi}{d\ln\xi}+3\Phi=0 \tag{2.11}$$

$$\frac{1}{\Psi}\frac{dF}{d\ln\xi}+(\Phi-\alpha)\frac{d\Phi}{d\ln\xi}+\frac{1}{\Psi}\frac{dG}{d\ln\xi}+\frac{1}{\Psi}\frac{dL}{d\ln\xi}+\frac{2}{\Psi}(F+G+L)$$

$$+\Phi(\Phi-1)=0 \tag{2.12}$$

$$\frac{dF}{d\ln\xi}+Y(\Psi,F,G)\frac{d\ln\Psi}{d\ln\xi}+2F\left[1+\frac{\alpha-1}{\Phi-\alpha}\right]=0 \tag{2.13}$$

$$(\Phi-\alpha)\frac{dL}{d\ln\xi}+2L\frac{d\Phi}{d\ln\xi}+2L(4\Phi-1)=0 \tag{2.14}$$

$$G=\frac{K^2}{2}\Psi(\xi\Phi)'[|(\xi\Phi)'|-(\xi\Phi)'] \tag{2.15}$$

where $'$ denotes differentiation with respect to ξ and

$$Y(\Psi,F,G)=\frac{\alpha^2}{\xi^2}\left[\Pi'\Psi-\Pi\left(\frac{\Gamma'\Psi}{\Gamma-1}+1\right)\right]-F\left(\frac{\Gamma'\Psi}{\Gamma-1}+\Gamma\right)-(\Gamma-1)G \tag{2.16}$$

and the transformed boundary conditions are

$$\Psi(1)=\beta,\ \Phi(1)=\left(1-\frac{1}{\beta}\right),F(1)=\left(1-\frac{1}{\beta}-\frac{c_0\beta^2}{2}\right),$$

$$L(1)=\frac{c_0\beta^2}{2}\text{ and }G(1)=0 \tag{2.17}$$

The numerical solution of equations (2.11)−(2.15) will be obtained by considering two cases. Firstly considering the regions where the viscosity is absent and secondly when it is present. Thus the flow field defines two regions based on the gradient of the term $(\xi\Phi)$. The region $(\xi\Phi)'\leq 0$ means that the viscous effect is present in the flow field that comprises of transition flow field between the undisturbed medium and shock front. Thus the equation (2.15) may be rewritten as follows,

$$\frac{d\Phi}{d\xi}=\frac{-1}{\xi K\left(\frac{\Psi}{G}\right)^{\frac{1}{2}}}-\frac{\Phi}{\xi} \tag{2.18}$$

For the region $(\xi\Phi)' > 0$, the viscosity term of equation (2.15) is zero (*i.e.* $G = 0$) and the remaining equations defining the flow can be written in matrix form for convenience as

$$\begin{pmatrix} \Phi-\alpha & 1 & 0 & 0 \\ 0 & \Phi-\alpha & \frac{1}{\Psi} & \frac{1}{\Psi} \\ Z & 0 & 1 & 0 \\ 0 & 2L & 0 & \Phi-\alpha \end{pmatrix} \begin{pmatrix} \frac{d\ln\Psi}{d\ln\xi} \\ \frac{d\Phi}{d\ln\xi} \\ \frac{dF}{d\ln\xi} \\ \frac{dL}{d\ln\xi} \end{pmatrix} = \begin{pmatrix} -3\Phi \\ -\frac{2}{\Psi}(F+L)-\Phi(\Phi-1) \\ -2F\left[1+\frac{\alpha-1}{\Phi-\alpha}\right] \\ -2L(4\Phi-1) \end{pmatrix} \tag{2.19}$$

where

$$Z(\Psi,F) = \frac{\alpha^2}{\xi^2}\left[\Pi'\Psi - \Pi\left(\frac{\Gamma'\Psi}{\Gamma-1}+1\right)\right] - F\left(\frac{\Gamma'\Psi}{\Gamma-1}+\Gamma\right) \tag{2.20}$$

The numerical solution procedure involves in writing equation (2.19) as follows:

$$\frac{d\Psi}{d\xi} = \frac{\Psi\triangle_1}{\xi\triangle}, \frac{d\Phi}{d\xi} = \frac{\triangle_2}{\xi\triangle}, \frac{dF}{d\xi} = \frac{\triangle_3}{\xi\triangle}, \frac{dL}{d\xi} = \frac{\triangle_4}{\xi\triangle} \tag{2.21}$$

where

$$\triangle = (\Phi-\alpha)\left[(\Phi-\alpha)^2 + \frac{1}{\Psi}(Z-2L)\right] \tag{2.22}$$

$$\triangle_1 = (\Phi-\alpha)\left[\Phi(\Phi-1) - 3\Phi(\Phi-\alpha) - \frac{2}{\Psi}(L+F)\frac{\alpha-1}{\Phi-\alpha}\right] \tag{2.23}$$

$$\triangle_2 = (\Phi-\alpha)\left[\tfrac{2}{\Psi}\{F(\alpha-1)-L(\Phi-\alpha)\} - \Phi(\Phi-1)(\Phi-\alpha) + \tfrac{2L}{\Psi}(4\Phi-1) - \tfrac{3\Phi Z}{\Psi}\right]$$

(2.24)

$$\triangle_3 = (\Phi-\alpha)\left[3\Phi Z(\Phi-\alpha) - \Phi(\Phi-1) - \tfrac{2}{\Psi}(F+L) + \tfrac{2LZ(\Phi-1)}{\Psi(\Phi-\alpha)} + 2F\left(1+\tfrac{\alpha-1}{\Phi-\alpha}\right)\left\{\tfrac{2L}{\Psi} - (\Phi-\alpha)^2\right\}\right]$$

(2.25)

$$\triangle_4 = 2L(\Phi-\alpha)\left[\Phi(\Phi-1) + \tfrac{2}{\Psi}\{L - F\tfrac{\alpha-1}{\Phi-\alpha}\} - \tfrac{Z(\Phi-1)}{\Psi(\Phi-\alpha)} - (\Phi-\alpha)(4\Phi-1)\right]$$

(2.26)

3. Solution Procedure

The solution procedure involves the following.

(a) Evaluation of β the measure of stock strength for the considered non-idealness parameters.

(b) Solutions of the transformed system of differential equations with and without viscosity.

3.1. Evaluation of β

The two EOS of Mie-Grunesien type, Royce [19], van dar Waals [22] are considered:

(a) putting $\Gamma(\Psi) = \Gamma_0 + 1 - d(1 - \frac{1}{\Psi})$ and $\Pi(\Psi) = 0$ in equation (2.7), the Royce EOS can be written as,

$$p = \rho e \left[\Gamma_0 - -d(1 - \frac{1}{\Psi})\right] \tag{3.1}$$

where $d > 0$ is an arbitrary constant and Γ_0 is non-ideal parameter. Again

(b) putting $\Gamma(\Psi) = 1 + \frac{\gamma-1}{1-b\Psi}$ and $\Pi = \left[1 - \frac{\gamma-1}{1-b\Psi}\right] a\Psi^2$ in equation (2.7) the van der Waals EOS can be written as,

$$p = \left(\frac{\gamma - 1}{1 - B\rho}\right)(\rho e + A\rho^2) - A\rho^2 \tag{3.2}$$

where $a = A\rho_0^2$, $b = B\rho_0$, e denotes the specific internal energy, γ is the ratio of specific heats ($\gamma > 1$), and the quantities A, B are the van der Waals gas constants for molecular cohesive forces and finite size of molecules ($A \geq 0$and $0 \leq B < \frac{1}{\rho}$) respectively. Substituting equations (3.1) and (3.2) in equation (2.8), we obtain the following two biquadratic equations in terms of β respectively.

$$M(\beta) \equiv c_0\beta^4 + (\Gamma_0 - d)\beta^3 + (3d - 2 - 2\Gamma_0)\beta^2 + (2 - 3d + \Gamma_0)\beta + d = 0$$

(3.3)

$$N(\beta) \equiv b(2a - c_0)\beta^4 + \{c_0 - a(4 - 2\gamma)\}\beta^3 + (2b + \gamma - 1)\beta^2 - 2(\gamma + b)\beta + (\gamma + 1) = 0$$

(3.4)

Using MATLAB these equations are solved for β corresponding to the constants $(a, b, c_0,$
d, γ and $\Gamma_0)$. Descarte's rule of signs suggest that the polynomial $M(\beta)$ has two negative and two positive roots whereas $N(\beta)$ has one negative and three positive roots. This can also be seen from the solution curves (Figs. 1 and 2). We observed from these figures that there is always one real root $(\beta = 1)$ irrespective of the constants considered. This corresponds to case of no magnetic effect $(c_0 = 0)$. Neglecting the negative roots subsequent computations are performed.

3.2. Solutions of the transformed equations

The solution of the non-linear system of ordinary differential equations is obtained by considering the two cases, (i) without viscosity $(K = 0)$ and (ii) with viscosity $(K \neq 0)$.

3.3. Numerical solution without viscosity $(K = 0)$

To obtain the solution without viscosity with the known values of $\beta, \Gamma_0$and γ the system of equations (2.21) are solved numerically where α is unknown. Substituting the boundary conditions (2.17) into the equations (2.21) and using the method of shock fitting we obtain the following simplified equations

(3.5) $$P_1\alpha^2 + Q_1\alpha + R_1 = 0 \qquad \text{(Royce EOS)}$$

(3.6) $$P_2\alpha^2 + Q_2\alpha + R_2 = 0 \qquad \text{(van der Waals EOS)}$$

where α_i s are roots of equations (3.5) and (3.6) and

$$P_1 = 2[d\beta^3 + (\Gamma_0 - d)\beta^4]$$

$$
\begin{aligned}
Q_1 &= 4[d\beta^2 + (\Gamma_0 - 2d)\beta^3 - (\Gamma_0 - d)\beta^4] \\
R_1 &= 2d^2 + 2d(2\Gamma_0 - 3d + 1)\beta + 2[(\Gamma_0 - 3d)(\Gamma_0 - d + 1) + (\Gamma_0 - d)]\beta^2 \\
&\quad +[c_0 d^2 - 2(\Gamma_0 - d)(\Gamma_0 - d + 1) + 2(3d - 2\Gamma_0)]\beta^3 + 2[(\Gamma_0 - d)(1 + dc_0) \\
&\quad -dc_0]\beta^4 + c_0(\Gamma_0 - d)(\Gamma_0 - d + 1)\beta^5 \\
P_2 &= 2\beta^2 + [a(4 - 2\gamma) - 4b]\beta^3 + [ab(2\gamma - 8) + 2b^2]\beta^4 + 4ab^2\beta^5 \\
Q_2 &= 4\beta - (8b + 4)\beta^2 + (4b^2 + 8b)\beta^3 - 4b^2\beta^4 \\
R_2 &= 2(1 + \gamma) - 2(2 + \gamma)(1 + b)\beta + 2[1 + (4 + \gamma)b + b^2]\beta^2 + \\
&\quad [(\gamma - 2)c_0 - 4b - 4b^2]\beta^3 + [(4 - \gamma)bc_0 + 2b^2]\beta^4 - 2c_0 b^2\beta^5
\end{aligned}
$$

The roots of the biquadratic equations (3.3), (3.4) and the quadratic equations (3.5), (3.6) for different non-ideal parameters are shown in Tables 1 and 2.

3.4. Numerical solution with Viscosity (K)

The presence of viscosity is expected to damp the amplitude of oscillations near the discontinuities in the physical quantities and thereby the Rankine-Hugoniot conditions do not show any special significance in the viscosity formalism. The system of equations (2.11) - (2.14) and (2.18) are solved numerically with the known values of β, Γ_0, γ, α (obtained previously) and viscosity K $(= 0.003439, 0.0349$ and $0.349)$ [21]. To integrate the set of non-linear ordinary differential equations without and with viscosity we use Runge-Kutta fourth order method with small step size. The integration is carried out in the range, $1 \leq \xi < \infty$ Starting the integration with a known value of β and α (α is evaluated corresponding to every β iteratively), shown in Tables 3.1 and 3.2, the whole solution procedure is repeated until the shock conditions are satisfied within the desired accuracy.

4. Results and discussion

In this paper, the entire computational work has been carried out using MATLAB. Numerical calculations are performed for the values of non-ideal parameters $d = 0.1, 0.3, 0.5, 0.7, 1.0$; $c_0 = 0.02, 0.05$; $b = 0.0004, 0.001,$ $0.005, 0.01, 0.03$, $\Gamma_0 = 1.78$ and 2.12 and $\gamma = 1.4, 1.6$. The values of similarity exponent α for different values of β in the case of Royce and van der Waals EOS are listed in Tables 1 and 2 respectively. The variations of non-dimensional density, shock velocity, pressure and magnetic pressure with ξ

		$\Gamma_0 = 1.78$		$\Gamma_0 = 2.12$	
d	c_0	β	α	β	α
0.1	0.02	2.0616	1.32738	1.89160	1.33130
	0.05	1.9315	1.28273	1.78867	1.28039
0.3	0.02	2.1284	1.31746	1.93417	1.32320
	0.05	1.9829	1.27537	1.82234	1.27433
0.5	0.02	2.2094	1.30624	1.98357	1.31420
	0.05	2.0436	1.26708	1.86077	1.26760
0.7	0.02	2.3100	1.29336	2.04184	1.30411
	0.05	2.1167	1.25770	1.90523	1.26008
1.0	0.02	2.5206	1.26985	2.15300	1.28631
	0.05	2.2613	1.24099	1.98726	1.24694

Table 3.1: Similarity exponent α for Royce EOS when $\Gamma_0 = 1.78, 2.12$ (Rounded to 5 digits)

		$a = 0.0025$				$a = 0.0075$			
		$\gamma = 1.4$		$\gamma = 1.6$		$\gamma = 1.4$		$\gamma = 1.6$	
b	c_0	β	α	β	α	β	α	β	α
0.0004	0.02	4.76932	1.28941	3.75301	1.30083	5.10068	1.26749	3.85936	1.29204
	0.05	3.74624	1.29955	3.16116	1.29411	3.89914	1.28819	3.22478	1.28893
0.001	0.02	4.76157	1.28987	3.74788	1.30124	5.08995	1.26821	3.85327	1.29259
	0.05	3.74301	1.29974	3.15846	1.29433	3.89516	1.28848	3.22168	1.28922
0.005	0.02	4.71012	1.29296	3.71393	1.30404	5.01922	1.27301	3.81306	1.29624
	0.05	3.72142	1.30106	3.14044	1.29578	3.86863	1.29045	3.20107	1.29113
0.01	0.02	4.64644	1.29694	3.67204	1.30758	4.93287	1.27906	3.76379	1.30084
	0.05	3.69427	1.30279	3.11794	1.29765	3.83541	1.29301	3.17541	1.29357
0.03	0.02	4.39947	1.31396	3.51064	1.32218	4.60935	1.30386	3.57709	1.31937
	0.05	3.58427	1.31055	3.02839	1.30565	3.70229	1.30415	3.07413	1.30382

Table 3.2: Similarity exponent α for van der Waals EOS, when $\gamma = 1.4, 1.6$

for Royce and van der Waals EOS in the absence of viscosity ($K = 0$) and with viscosity ($K = 0.00349, 0.0349$ and 0.349) are investigated in detail and are shown in Figures (3) - (10). The results of the study in both EOSs (Royce and van der Waals) are summarized as follows.

The increase in the non-idealness parameters d, a and b, has effect on the measure of shock strength β. It is notable that increase in magnitude of β in case of Royce EOS and decrease in the van der Waals EOS respectively (see Tables 1 and 2).

In the absence of viscosity ($K = 0$), from Figures 3(a)-3(d) it is observed that the density, velocity, pressure, and magnetic pressure distributions for Royce EOS decreases with the increasing values of d (non-idealness parameter) and β (measure of shock strength). Whereas in the case of van der Waals EOS, the flow variables density, velocity, and pressure increase with an increasing values of non-idealness parameter (b), and for decrease in measure of shock strength (β) as shown in Figures 7(a) - (d). In both the EOS under consideration the flow variables developed sharp edge profiles. This can be attributed to the excitation of oscillations in molecules through shock front. The change in magnetic pressure is negligible with change of non-idealness parameter (b). This phenomenon is observed to be more prominent in case of van der Waals EOS than Royce EOS. Similar trend in the velocity and density profiles were reported by [11, 16] respectively.

It is very important to observe that in the presence of viscosity formalism ($i.e, K \neq 0$) the profiles of the flow field could lead to continuous shock flow fields in which the sharp edged continuous profiles at the shock wave reduce and change to smooth curves. Flow variables (physical parameters) changed rapidly, but smoothly for both EOS. It is to be noted that the effect on flow variables (physical parameters) in the medium of van der Waals EOS is appreciable for small values of non-idealness parameter (b), while for large values of non-idealness parameter (b), it is very small. Similar trend in the pressure profiles were reported by [5] and density profiles by [5, 16].

It is observed that in the presence of non-idealness parameters d and b along with the introduction of artificial viscosity ($K = 0.00349$) during the numerical integration process the nature of the profiles of both the EOS

change from being sharp edged to smooth curves (Figures 4(a) - (d) and 8(a) - (d)). The smoothness in the flow parameters further improved by increasing the value of viscosity *i.e.*, $K = 0.0349$ to 0.349 in both the EOS (Figures 4, 5 (a) - (d) and Figures 9, 10 (a) - (d)). With the non-idealness parameter $d(= 0.1, 0.3, 0.5)$ and $K = 0.0349$, from Figures 5(a) - (d) for Royce EOS the density, velocity, pressure and magnetic profiles gradually increase with increase in ξ and decrease slowly and become constant. This behavior continues to remain the same with sharp edges becoming smoother with increase in the value of $K(= 0.349)$ (Figures 6(a) - (d)). Thus we conclude that along with the non-idealness parameters and with the introduction of artificial viscosity ($K = 0.00349, 0.0349$ and 0.349) the excitation of oscillations in the molecules dampen and the smoothness in the profiles increases. With the non-idealness parameter $b(= 0.001, 0.005, 0.01)$ and $K = 0.0349$, from Figures 9(a) - (d) for van der Waals EOS the density, velocity, pressure and magnetic profiles gradually increase with increase in ξ and slowly and become constant. This behavior remains unaltered with the value of $K > 0.349$ (Figures 10(a) - (d)).

It is observed that spread of flow variables increases with increase in the range of the non-idealness parameter (b) and fixed values of viscosity parameter (K). Thus, the thickness of MHD shock front increases with increase in the value of non-idealness parameter (b). The thickness of MHD shock wave depends only on its strength and is constant with increase in reduced distance (ξ) . However, the increase in the thickness of shock front with increase in the non-idealness parameter (b) is more notable for certain range of values of viscosity parameter (K) for both EOS of Royce and van der Waals.

Numerical computations revealed that the change in the flow variables with the non-idealness parameters (d), and (b) is constant and independent of large values of viscosity parameter (K) for Royce and van der Waals EOS respectively. Thus artificial viscosity has no effect along a wave front of constant phase. This is because the velocity component tangential to a shock front is continuous in the limit of arbitrary grid refinement in this direction. This type of behavior is called wave front invariance.

In particular, we observed that for smaller values of magnitude of viscosity parameter (K) the effect on flow variables velocity, pressure are constant initially with the increase in ξ and decreases more rapidly with increas-

ing values of non-idealness parameter (b) and fixed values of non-idealness parameter (a) in the EOS of van der Waals. Also it is observed that the thickness of MHD shock front is maximum for small values of non-idealness parameter (b), which increases more with increasing values of non-idealness (a) and fixed values of non-idealness parameter (b).

We concluded that artificial viscosity could distinguish between shock-wave and adiabatic compression. It vanishes for uniform compression and rigid rotation and also vanishes along a surface of constant phase. Along such a surface the velocity field has a constant magnitude, and is also continuous, but may vary in direction. Moreover, artificial viscosity produce forces that go to zero continuously as compression goes to zero for expansion, so that latter is a reversible process.

4.1. Conclusions

In this work MATLAB is used for the entire computational work and the values of the non-ideal parameters $d = 0.1, 0.3, 0.5, 0.7, 1.0, c_0 = 0.02, 0.05$; $\Gamma_0 = 1.78, 2.12, \gamma = 1.4, 1.6; K = 0.00349, 0.0349, 0.349$ and $b = 0.0004$, $0.001, 0.005, 0.01, 0.03$ are used. The values of similarity exponent α for different values of β for Royce EOS and van der Waals EOS are evaluated. The conclusions of the study are summarized as follows.

(1) It is noted that the increase in the non-idealness parameters d, a and b, have effect on the measure of shock strength β *i.e.*, increase in magnitude of β in case of Royce EOS and decrease in the van der Waals EOS respectively.

(2) In the presence of non-idealness parameters and in the absence of viscosity ($K = 0$), the density, velocity, pressure, and magnetic pressure distributions for Royce EOS observed to decrease with the increasing values of non-idealness parameter (d), and for increasing values of measure of shock strength (β).

(3) In the case of van der Waals EOS, the flow variables density, velocity, and pressure increase with an increasing values of non-idealness parameter (b), and for decrease in measure of shock strength (β).

(4) In both the EOS under consideration it is observed that the flow variables have sharp edge profiles. The change in magnetic pressure is negligible in case of van der Waals EOS than Royce EOS.

(5) It is notable that in the presence of non-idealness parameters d and b and with the introduction of artificial viscosity $(K = 0.00349, 0.0349, 0, 349)$ during the numerical integration process the nature of the profiles of both the EOS change from being sharp edged to smooth curves.

(6) It is observed that the large value of artificial viscosity has no effect along a wave front of constant phase because the velocity component tangential to a shock front is continuous in the limit of arbitrary grid refinement in this direction.

(7) With the non-idealness parameter $b(= 0.001, 0.005, 0.01)$ and $K = 0.0349$, for van der Waals EOS the density, velocity, pressure and magnetic profiles gradually increases with increase in ξ and slowly and become constant. This behaviour remains unaltered with the value of $K > 0.349$.

(8) We conclude that with the non-idealness parameters and with the introduction of artificial viscosity ($K = 0.00349, 0.0349$ and 0.349) the excitation of oscillations in the molecules dampen and the smoothness in the profiles increases.

(9) It is observed that spread of flow variables increases with increase in the range of the non-idealness parameter (b) and fixed values of viscosity parameter (K).

(10) The thickness of MHD shock front increases with increase in the value of non-idealness parameter (b). It is observed that the thickness of MHD shock wave depends only on its strength and is constant with increase in reduced distance (ξ).

(11) It is observed that for smaller values of viscosity parameter (K) the effect on flow variables is constant initially with the increase in ξ and decreases more rapidly with increasing values of non-idealness parameter (b) and fixed values of non-idealness parameter (a) in the EOS of van der Waals. Also it is observed that the thickness of MHD shock front is maximum for small values of non-idealness parameter (b), which increases more with an increasing values of non-idealness parameter (a) and fixed values of non-idealness parameter (b).

(12) We conclude that artificial viscosity distinguishes between shock-wave and adiabatic compression. It vanishes for uniform compression and

rigid rotation and also vanishes along a surface of constant phase. Along such a surface the velocity field has a constant magnitude, and is also continuous, but may vary in direction.

Acknowledgement

The authors acknowledges with thanks the financial and technical support provided by Department of Science and Technology, New Delhi, India, through Inspire fellowship (IF110071).

References

[1] G. Ali, J.K. Hunter, *Wave interactions in magnetohydrodynamics*, Wave Motion, 27, pp. 257-277, (1998).

[2] I. Ballai, E. Forgacs-Dajka, A. Marcu, *Dispersive shock waves in the solar wind*, Astronomische Nachrichten, 328 (8), pp. 734-737, (2007).

[3] J. Blazek, Computational Fluid Dynamics: Principles and Applications, Elsevier, Amsterdam, (2001).

[4] E. J. Caramana, M. J. Shashkov, P. P. Whalen, *Formulations of artificial viscosity for multi-dimensional shock wave computations*, J. Comput. Phys., 144 (1), pp. 70-97, (1998).

[5] A. V. Chikitkin, B. V. Rogov, G. A. Tirsky, S. V. Utyuzhnikov, *Effect of bulk viscosity in supersonic flow past spacecraft*, Applied Numerical Mathematics, doi: 10.1016/j.apnum.2014.01.004 (2014).

[6] R.F. Chisnell, *An analytic description of converging shock waves*, J. Fluid. Mech., 354, pp. 357-375, (1998).

[7] V. Genot, *Analytical solutions for anisotropic MHD shocks*, Astro. Phys. Space Sci. Trans., 5, pp. 31-34, (2009).

[8] W. Gretler, R. Regenfelder, *Similarity solution for laser-driven shock waves in a particle-laden gas*, Fluid Dynamics Research, 28 (5), pp. 369-382, (2001).

[9] P. Hafner, *Strong convergent shock waves near the center of convergence: A power series solution*, SIAM J. Appl. Math., 48 (6), pp. 1244-1261, (1998).

[10] P. M. Jordan, M. R. Meyer, A. Puri, *Causal implications of viscous damping in compressible fluid flows*, Phys. Rev., E. 62, pp. 7918 - 7926, (2000).

[11] V. Khodadad, N. Khazraiyan, *Numerical modeling of ballistic penetration of long rods into ceramic/metal armors*, 8th International LS-DYNA Users Conference-Drop/Impact Simulations, 14, pp. 39-50, (2004).

[12] V. P. Korobeinikov, *Problems in the theory of point explosion in gases*, Providence, American Mathematical Society, Rhode Island (1976).

[13] N. P. Korzhov, V. V. Mishin, V.M. Tomozov, *On the viscous interaction of solar wind streams*, Soviet Astronomy, 29, pp. 215-218, (1985).

[14] L.D. Landau, E. M. Lifshitz, Fluid Mechanics, Pergamon press, New York (1987).

[15] R. Lazarus, R. D. Richtmyer, *Similarity solutions for converging shocks*, Technical report LA- 6823-MS. Los Alamos Scientific Laboratory (1977).

[16] W. H. Lee, P.P. Whalen, *Calculation of shock problems by using four different schemes*, International Conference on Numerical Methods for Transient and Coupled Problems. Venice, Italy (1984).

[17] A. A. Maslov, S. G.Mironov, A. N. Kudryavtsev, T. V. Poplavskaya, I.S. Tsyryulnikov, *Wave process in a viscous shock layer and control of fluctuations*, J. Fluid Mech., 650, pp. 81-118, (2010).

[18] J. A. Orta, M.A. Huerta, G. C. Boynton, *Magnetohydrodynamic shock heating of the solar corona*, The Astrophysical Journal., 596, pp. 646-655, (2003).

[19] A. Ramu, M. P. Ranga Rao, *Converging spherical and cylindrical shock waves*, J. Eng. Math. 27 (4), pp. 411-417, (1993).

[20] A. Ramu, N. Dunna, D. K. Satpathi, *Numerical study of shock waves in non-idea magnetogasdynamics*, Journal of Egyptian Mathematical Society, 24 (1), pp. 116-124 (2016).

[21] L. Richard, Similarity solutions for a spherical shock wave, J. Appl. Phys., 26 (8), pp. 954-960, (1955).

[22] V. D. Sharma, R. Arora, *Similarity solutions for strong shocks in an ideal gas*, Stud. Appl. Math. 114 (4), pp. 375-394, (2005).

[23] K. P. Stanyukovich, *Unsteady motion of Continuous Medi,*. Pergamon Press, New York (1960).

[24] G. I. Taylor, *The formation of a blast wave by a very intense explosion-I and II: The atomic explosion of 1945*, Proc. Roy. Soc., London, 201 (1065), pp. 159-186, (1950).

[25] J. Von Neumann, R.D. Richtmyer, *A method for the numerical calculation of hydrodynamic shocks*, J. Appl. Phys. , 21 (3), pp. 232-237, (1950).

[26] G. B.Whitham, *Linear and Non-linear Waves*. John Wiley & Sons, New York, (1974).

[27] Ya. B.Zeldovich, Y.P. Raizer, *Physics of Shock waves and High-Temperature Hydrodynamic Phenomenon*. Vol. II., Academic Press, New York, (1966).

[28] K. Zumbrun, *The refined inviscid stability condition and cellular instability of viscous shock waves*, Physica D: Nonlinear Phenomena., 239 (13), pp. 1180-1187, (2010).

Narsimhulu Dunna
Department of Mathematics
Birla Institute of Technology and Science - Pilani,
Hyderabad - Campus
Jawahar Nagar Shameerpet,
INDIA
e-mail : narsimha.maths@gmail.com

Addepalli Ramu
Department of Mathematics
Birla Institute of Technology and Science - Pilani,
Hyderabad - Campus
Jawahar Nagar Shameerpet,
INDIA
e-mail : aramu@hyderabad.bits-pilani.ac.in

and

Dipak Kumar Satpathi
Department of Mathematics
Birla Institute of Technology and Science - Pilani,
Hyderabad - Campus
Jawahar Nagar Shameerpet,
INDIA
e-mail : dipak@hyderabad.bits-pilani.ac.in

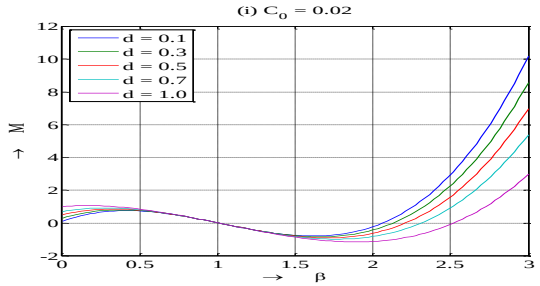

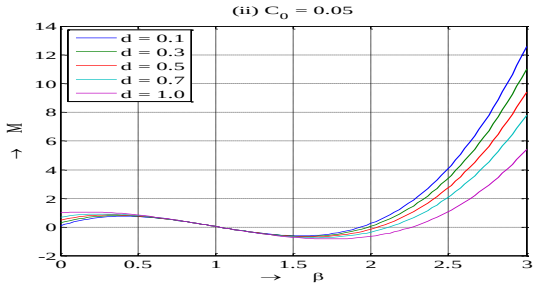

Figure 1: Graphical approach of $M(\beta)$ for Roye's EOS when $\Gamma_0 = 1.78$ and various values of d

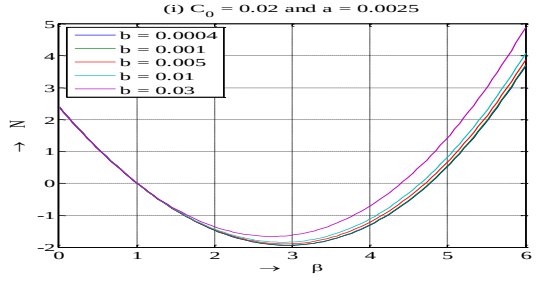

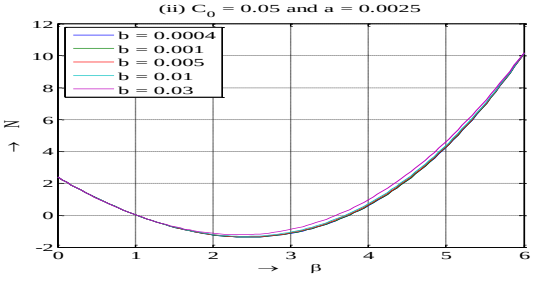

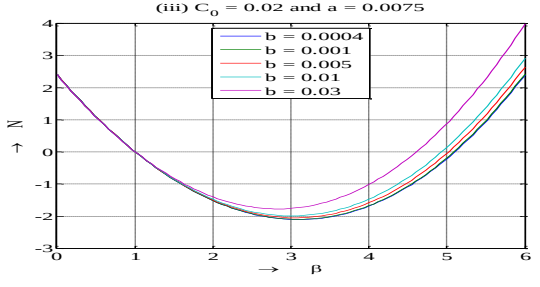

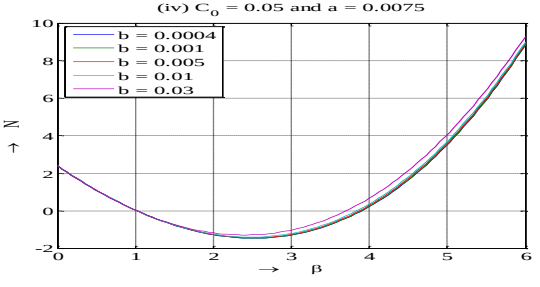

Figure 2: Graphical approach of $N(\beta)$ for van der Wall's EOS when $\gamma = 1.4$ and various values of b

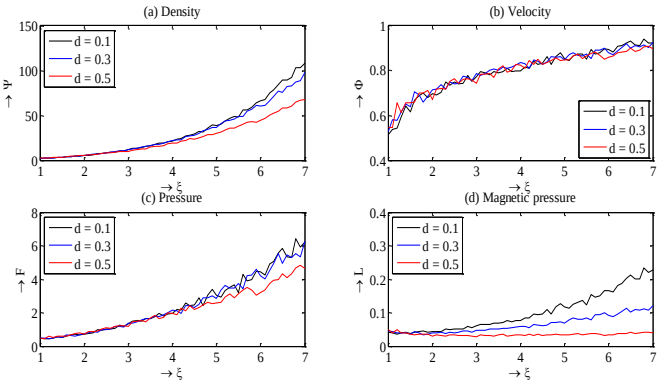

Figure 3. Profiles for Roye's EOS when $k = 0$

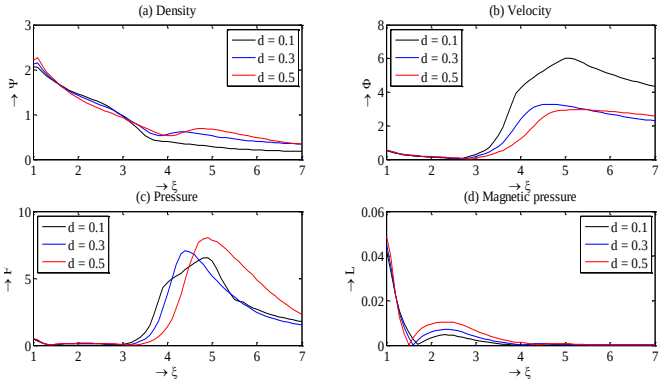

Figure 4: Profiles for Roye's EOS when $k = 0.00349$

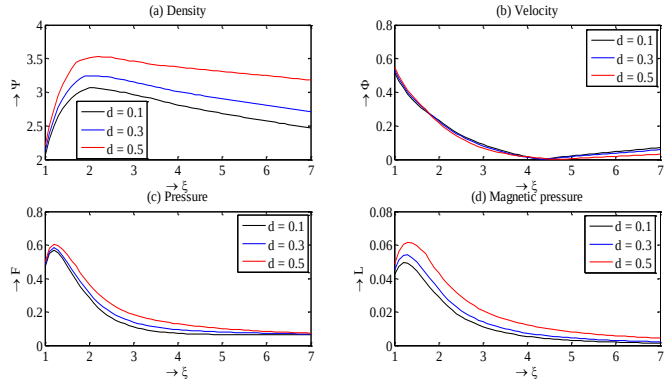

Figure 5: Profiles for Roye's EOS when $k = 0.0349$

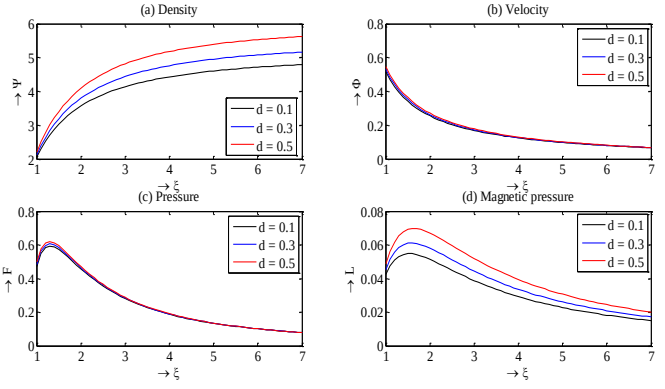

Figure 6: Profiles for Roye's EOS when $k = 0.349$

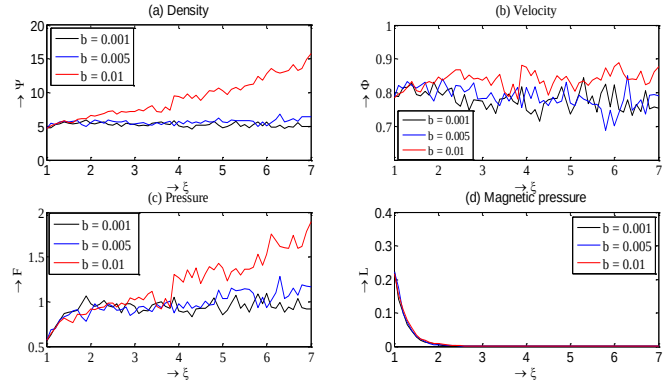

Figure 7. Profiles for van der Wall's EOS when $k = 0$

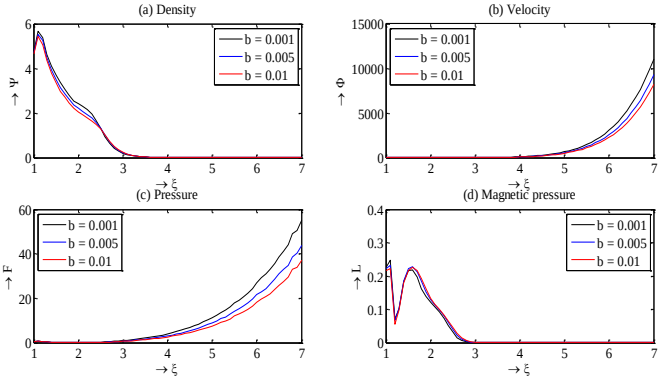

Figure 8. Profiles for van der Wall's EOS when $k = 0.00349$

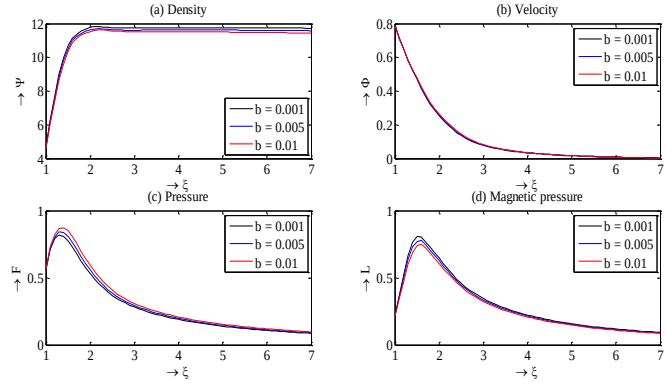

Figure 9. Profiles for van der Wall's EOS when $k = 0.0349$

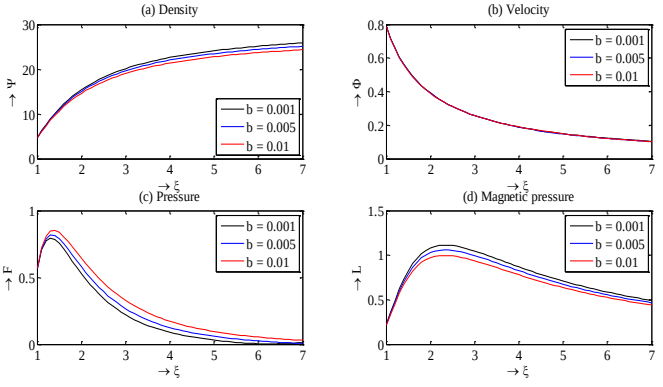

Figure 10. Profiles for van der Wall's EOS when $k = 0.349$